ATOLL RESEARCH BULLETIN

NO. 567

THE MICROBIAL COMMUNITIES OF THE MODERN MARINE STROMATOLITES AT HIGHBORNE CAY, BAHAMAS

BY

JOHN F. STOLZ, R. PAMELA REID, PIETER T. VISSCHER, ALAN W. DECHO, R. SEAN NORMAN, REBECCA J. ASPDEN, EMILY M. BOWLIN, JONATHAN FRANKS, JAMIE S. FOSTER, DAVID M. PATERSON, KRISTEN M. PRZEKOP, GRAHAM J.C. UNDERWOOD, AND LEE PRUFERT-BEBOUT

ISSUED BY
NATIONAL MUSEUM OF NATURAL HISTORY
SMITHSONIAN INSTITUTION
WASHINGTON, D.C., U.S.A.
JULY 2009

THE MICROBIAL COMMUNITIES OF THE MODERN MARINE STROMATOLITES AT HIGHBORNE CAY, BAHAMAS

BY

JOHN F. STOLZ,[1] R. PAMELA REID,[2] PIETER T. VISSCHER,[3] ALAN W. DECHO,[4] R. SEAN NORMAN,[4] REBECCA J. ASPDEN,[5] EMILY M. BOWLIN,[2] JONATHAN FRANKS,[1] JAMIE S. FOSTER,[6] DAVID M. PATERSON,[5] KRISTEN M. PRZEKOP,[3] GRAHAM J.C. UNDERWOOD,[7] AND LEE PRUFERT-BEBOUT[8]

ABSTRACT

An intensive multi-year field study of the modern marine stromatolites at Highborne Cay, Bahamas has identified a variety of microbial communities that colonize the stromatolite surfaces. They include both bacterial and diatom dominated communities. The "classic" microbial communities are those described by Reid et al. (2000). They include *Schizothrix* mats, dominated by *S. gebeleinii,* which trap and bind ooid sand grains (Type 1 mat); biofilm mats, composed of sulfate reducing bacteria, which form thin crusts of microcrystalline carbonate (Type 2 mat); and *Solentia* mats, dominated by coccoid endolithic *Solentia* species, which create cemented layers of fused sand grains (Type 3 mat). Another bacterial mat, termed "pudding mat" due to its pudding-like texture, is dominated by thin filaments of *Phormidium* sp. and single filaments of *S. gebeleinii*, but may also be colonized by a unique species of coccoid cyanobacterium related to *Cyanothece*. The diatom mats include stalked diatoms and tube diatoms. The stalked diatom mats form as a thin (1-3 mm) surface pink fuzz comprised of *Striatella unipunctata*, or a yellow fuzz that may develop into a thick (0.5-1 cm) yellow fur with *Licmophora remulus* and *Licmophora paradoxa*. The tube diatom mats, which occur as discrete pustules that may coalesce to create uniform blankets, are formed by naviculid – like tube diatoms. These different mat types recognized based on field descriptions and light microscopy also show distinct differences based on microbial fingerprinting and carbohydrate fractionation. Denaturing gradient gel electrophoresis (DGGE) analyses show similarities between stalked diatom mat types

[1]Department of Biological Sciences, Duquesne University, Pittsburgh PA 15282 USA, stolz@duq.edu
[2]Rosenstiel School of Marine and Atmospheric Science, Division of Marine Geology and Geophysics, University of Miami, 4600 Rickenbacker Causeway, Miami, FL 33149-1098, USA
[3]Department of Marine Sciences, University of Connecticut, 1080 Shennecossett Rd., Groton, CT 06340-6097, USA.
[4]Department of Environmental Health Sciences, Arnold School of Public Health, University of South Carolina, Columbia, SC 29208, USA.
[5]Sediment Ecology Research Group, Gatty Marine Laboratory, School of Biology, University of St Andrews, St Andrews, KY16 8LB, UK
[6]Department of Microbiology and Cell Science, University of Florida, Space Life Sciences Laboratory, Kennedy Space Center, Florida 32899
[7]Department Biological Sciences, University of Essex, Wivenhoe Park, Colchester, Essex CO4 3SQ, UK
[8]Exobiology Branch, NASA Ames Research Center, Moffet Field, CA, 94035, U.S.A.

Manuscript received 29 May 2009; revised 3 June 2009

and “classic” mat types 1 and 2; these mats cluster separately from tube diatom mats and pudding mats, which each form distinct clades. In addition, the carbohydrate fractions of classic mat types are composed mostly of structural extracellular polymeric secretions (EPS), whereas stalked diatom and pudding mats contain predominantly non-structural carbohydrates. Although the pudding mats and diatom communities can contribute to the trapping of ooids, the stabilization of the unconsolidated sediment ultimately requires binding by *S. gebeleinii*. The combination of carbohydrate composition and ability to rapidly rebound after burial result in the high erosion resistance exhibited by the “classic” mats. Conversely, the extremely sensitive nature of diatoms to burial results in the low erosion resistance of the diatom mats. Nevertheless, all may contribute to the biogenesis of the Highborne Cay stromatolites.

INTRODUCTION

The margins of Exuma Sound, Bahamas host the only known examples of stromatolites currently forming in open marine conditions, similar to those of many Precambrian platforms. The Highborne Cay locality has been under investigation for over a decade as the focus of numerous studies on the biogenesis and lithification of modern marine stromatolites and the communities and processes involved (e.g. see http://stromatolites.info for complete listing of publications). Previous reports (e.g. Reid et al., 2000; Visscher et al 2000; Macintyre et al., 2000) have emphasized the importance of three distinct prokaryotic microbial mat communities in the formation of Highborne Cay stromatolites: Type 1 mats, dominated by filamentous cyanobacteria; Type 2 mats, forming bacterial biofilms; and Type 3 mats characterized by endolithic coccoid cyanobacteria. Each community forms a distinct sedimentary structure, with Type 1 mats forming unconsolidated layers of trapped and bound sediment, Type 2 mats forming thin (20-60 μm thick) micritic crusts, and Type 3 mats forming cemented layers of fused sand grains. Stromatolite lamination was shown to result from a quasi-cyclical succession of the three mat types, with each layer in the subsurface representing a former surface mat (Reid et al., 2000). The Research Initiative on Bahamian Stromatolites (RIBS), comprised of an international and multidisciplinary team of scientists, initiated a study in 2003 to investigate and determine the possible environmental parameters that cause one mat type to shift to another, thereby creating stromatolite laminations. As part of this study, the stromatolites were monitored intensively for a 3 year time period (2005-07). During the course of the monitoring the “classic” Type 1, 2 and 3 mats were studied in more detail and several new surface mat communities were discovered (e.g., pudding mats, stalked diatom and tube-forming diatom mats). In the present paper we present a comprehensive description of the different microbial mat communities as characterized by gross anatomy, surface and cross-section morphology, oxygen profile, major species composition (e.g., light microscopy, fluorescence microscopy, confocal scanning laser microscopy, and transmission electron microscopy), molecular profiling (e.g., DGGE analysis), and carbohydrate composition (e.g., EPS). The conceptual model for stromatolite biogenesis as proposed by Reid et al. (2000) is then discussed in light of the new data.

Site Description

The field locality, Highborne Cay (76°49′W; 24°43′N), is an island in the northern Exuma Cays, Bahamas (Fig. 1). The climate is dominated by southeast to easterly trade winds averaging 10–15 knots. Sea-surface temperatures range from 20–28° C and the tidal variation is about 1 m. The water has a normal marine salinity (~35 ‰), and is saturated with respect to both aragonite and calcite (Littler et al., 2005). A fringing reef extends for about 2.5 km along the east, ocean-facing beach; the reef is best developed in the southernmost kilometer, where six distinct morphological zones are recognized: beach zone, thrombolite zone (microbialites with irregular internal microstructure), stromatolite zone (microbialites with laminated internal microstructure), reef flat zone, reef crest zone, and fore reef zone (Littler et al., 2005). The width of these zones is highly variable. Wave energy is driven primarily by local wind forcing, which increases in response to atmospheric disturbances (e.g., storms) typically lasting a few days (Eckman et al., 2008). The stromatolites, which require some degree of turbulence and water borne sediment, are protected from strong wave action by the shallow platform reef.

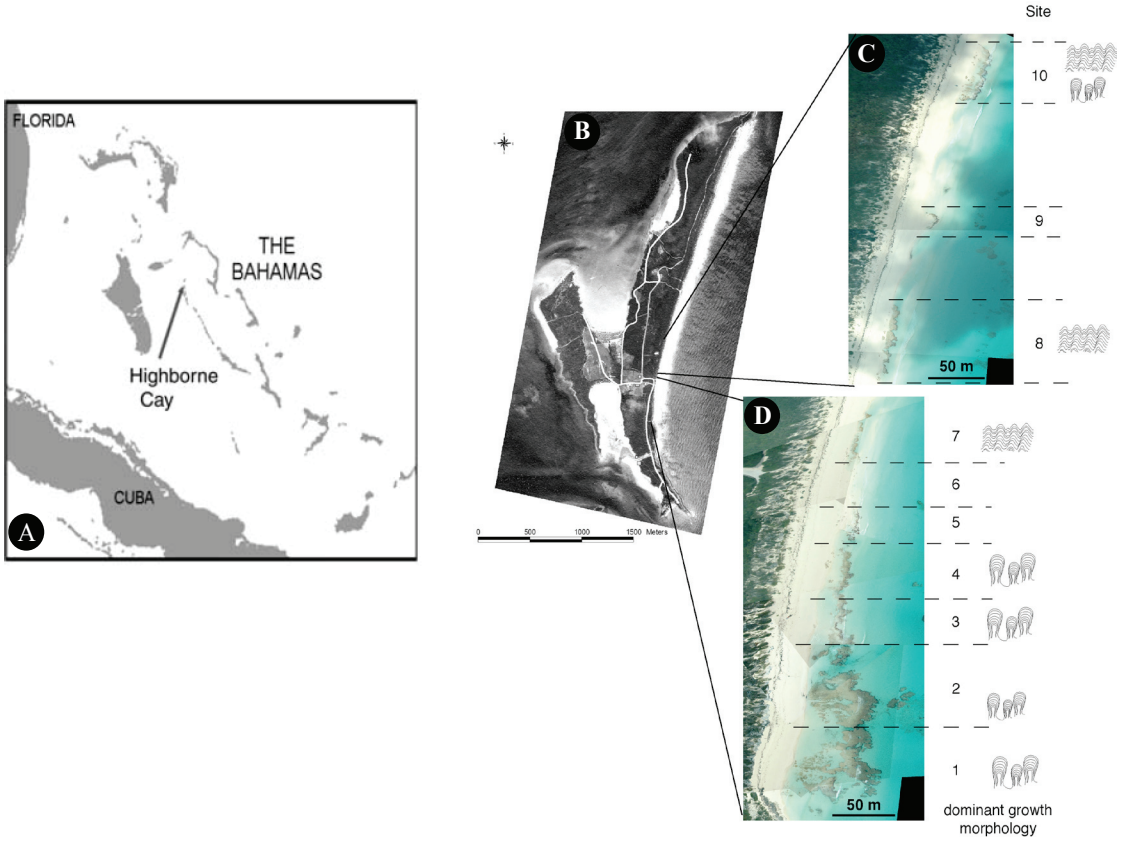

Figure 1. Field locality A) map of the Exumas, Bahamas showing location of Highborne Cay (arrow), B) aerial photograph of the island indication location of stromatolites. Designation of the 10 major sampling sites and dominant stromatolite morphologies C) sites 1 - 7, D) sites 8 -10. Modified with permission from Andres and Reid, 2006 and Ekman et al., 2008).

METHODS

Sample Collection and Documentation

Stakes were set up to delineate ten sites along the Highborne Cay reef track (Fig. 1). Each site was monitored at varying intervals (including nine research cruises) from 2003-2008 with daily to monthly visits during 2005-2007; mat types were recorded based on visual examination and sample collection. All samples were assigned a unique identification number, and distributed to various investigators for the analyses described below. A portion of each sample was cross-sectioned using a rock saw and photographed (both surface and cross section) to create a permanent reference record. Layers clearly distinguishable by either color or texture changes were sequentially identified and labeled on the reference photographs. These layers were then sub-sampled for microscopic observation.

Stereo, Light, Fluorescence, Confocal Scanning Laser, and Transmission Electron Microscopy

Macro- and micro-scale observations and photo-documentation were made using an Olympus SZX12 stereoscope with a C-2000Z digital camera and Olympus BX60 microscope with fluorescence (FM) and phase contrast (PCM) optics and a Q Color 3 digital camera. Confocal Scanning Laser Microscopy (CSLM) was conducted using a Leica TCS SP 2 (Leica Microsystems, Inc. Mannheim GR). Excitation was at 488 nm and three different ranges of emissions were used. Ooids were visualized by reflectance at 485-492 nm (blue). Two different emission ranges for chlorophyll *a* were used 644-722 nm (red) and 507-536 nm (green). Diatom stalks were visualized using a Lectin-FITC conjugate (Wustman et al., 1997). Samples for transmission electron microscopy (TEM) were prepared using the methods in Stolz et al. (2001). Thin sections were observed on a JEOL 100 CX transmission electron microscope with images taken with a SIA digital camera.

Oxygen Profiles

Depth profiles of oxygen were obtained with needle electrodes (0.6-0.8 mm outer diameter) (Visscher et al*.,* 1998, 2002). Triplicate measurements were made *in situ* using a tethered benthic lander (Unisense, Denmark). Measurements of depth profiles were then repeated dockside, using needle electrodes and a Unisense PA2000 picoammeter, at light intensities of 1800-2100 $\mu E.m^{-2}.s^{-1}$ and ambient temperature to confirm *in situ* measurements. The profiles presented in this paper are composites based on multiple profiles for each mat type; of the 28 profiles, the maximum observed concentrations and depth of O_2 penetration had a standard deviation within 9.6% of the mean for the same mat type. Values are discussed as % oxygen saturation as corrected for conductivity and temperature. Light measurements were made using a LiCor LI250A meter equipped with a LI-191 underwater quantum sensor.

Microbial Community Fingerprinting

Denaturing gradient gel electrophoresis (DGGE) analyses were conducted to obtain community fingerprints for a variety of mat types. Total community DNA was extracted from 100 mg of homogenized mat samples using the UltraClean Soil DNA kit (MoBio Laboratories, Inc., Carlsbad, CA). For DGGE analysis, a 193 bp sequence of the V3 region of the 16S rRNA genes was amplified using the primer set 341FGC and 534R (Muyzer et al., 1996). PCR products were purified using QIAquick PCR purification columns (Qiagen, Valencia, CA) and analyzed by DGGE using a Bio-Rad Dcode Universal Mutation Detection system (Bio-Rad Laboratories, Hercules, CA). Briefly, samples were run on 10% polyacrylamide gels with a denaturant gradient from 40% to 60%. Electrophoresis was carried out for 16 h at 70 V and 60°C. The gels were stained for 1 h with SYBR Green I DNA stain and imaged with a Storm fluorescence imaging system (GE Healthcare Biosciences, Piscataway, NJ). DGGE images were processed and normalized using BioNumerics software (Applied Maths, Inc., Austin, TX). DGGE fingerprints were compared using the band-based Dice coefficient of similarity followed by the construction of a dendrogram using the Unweighted Pair Group Method with Arithmetic Mean (UPGMA).

Carbohydrate Characterization and Fractionation

Fresh mats were sampled in the field, returned to the shipboard laboratory on the R/V Walton Smith and further processed. Carbohydrate extractions followed procedures modified from Bellinger et al. (2005) and Hanlon et al. (2006), as follows:

Colloidal Extracts, cLMW carbohydrate and cEPS (a). Incubation of fresh sediment slices for 20 min in 25‰ saline, was followed by centrifugation. The supernatant contains the colloidal carbohydrate (sensu Underwood et al., 1995). A subsample of the supernatant was precipitated in 70% alcohol overnight followed by further centrifugation. The supernatant of this contains the low molecular weight carbohydrate (cLMW) and the pellet the colloidal EPS (cEPS). Both samples were evaporated to dryness.

Hot water extract, HW (b). The sediment pellet from the saline extraction in 'a' was resuspended in deionized H_2O and incubated at 95°C for 1 h, then centrifuged. The supernatant contains hot-water extracted carbohydrate (HW). The supernatant was removed and evaporated to dryness. The pellet was used for hot bicarbonate extraction.

Hot bicarbonate extract, HB-LMW carbohydrate and HB-EPS. The sediment pellet from 'b' was resuspended in 0.5M NaOH, and incubated at 95°C for 1 h, then centrifuged. The hot bicarbonate solubilizes tightly bound and capsular EPS and structural stalks, e.g. from diatom stalks or cyanobacterial sheaths. The supernatant (containing the solubilized polymers) was precipitated in 70% alcohol overnight followed by further centrifugation. The resulting supernatant contains the low molecular weight carbohydrate (HB- LMW) and the pellet is HB-EPS. Both samples were evaporated to dryness.

These procedures result in five sediment carbohydrate fractions: two specific EPS fractions (defined as EPS by the precipitation step, cEPS and HB-EPS), and three carbohydrate fractions, cLMW, HW and HB-LMW. All data were expressed as μg glucose equivalents cm^{-2}, normalized to a 1 mm deep slice of biofilm.

Sediment chlorophyll *a* (Chl *a*) was measured on freeze dried mat samples (approx. 200 mg dry weight), extracted in 1.5 mL 100% acetone, with absorbance measured at λ of 630, 647, 664, and 750 nm (Underwood and Kromkamp, 1999). Concentrations were calculated to μg Chl *a* cm^{-2}, normalized to a 1 mm deep slice of biofilm.

RESULTS

Major Mat Types

Microbial mat communities on the stromatolite surfaces were characterized based on morphology (i.e., smooth, pustular, knobby, mushroom-shaped, fuzzy, furry), color (i.e., white, caramel, green, yellow, pink), hardness (i.e., soft, firm, brittle, crusty, hard), and dominant organisms. Four major groups were distinguished based on these characteristics: "classic" mats ("classic" designates mat types described by Reid et al., 2000), stalked diatom mats, tube diatom mats, and pudding mats (Table 1). As is the case for the "classic" mats, they may represent different stages in stromatolite biogenesis and may be present at varying abundance at different times of the year (Table 2). Each of the major mat types are described in detail below.

Table 1: Stromatolite mat types at Highborne Cay and their general characteristics.

Mat Type	Field Designation	Morphology	Color	Hardness	Dominant organisms
"Classic" Mats	clean smooth mats				
Schizothrix Mats (Type 1)		smooth	White, tan, pale green	firm	*Schizothrix gebeleinii*
Biofilm Mats (Type 2)		smooth	white	Soft to brittle	sulfate red. bac. *S. gebeleinii*
Solentia Mats (Type 3)		smooth	white	hard	*Solentia* spp., *S. gebeleinii* *Oscillatoria* spp. *Microcoleus* spp.
Stalked Diatom Mats	yellow fuzz, pink fuzz, yellow fur	fuzz to fur	yellow, pink	soft	*Striatella unipunctata, Licmorpha* spp.
Tube Diatom Mats	stringy pustules, pustular blanket	discrete pustules to pustular blanket	white	soft	Naviculid tube diatoms
Pudding Mats	pale pudding, coccoid pudding	smooth mounds	white to pale green	soft to firm	*Phormidium* sp. *S. gebeleinii* *Cyanothece* sp.

Table 2: Annual occurrence of mat types (A, abundant, C, common, R, rare, N, not seen).

Mat Type	Winter (Jan, F, Mar)	Spring (Apr, May, Jun)	Summer (Jul, Aug, Sep)	Fall (Oct, Nov, Dec)
"Classic"				
Type 1 mat	C	C	C	C
Type 2 mat	R	R	C	R
Type 3 mat	A	A	R	R
Yellow Fur	R	R	A	A
Tube diatom mat	A	R	C	A
Pudding mat	N	N	C	R

"Classic" Mats

The "Classic" mats are informally referred to in the field as "smooth clean mats", reflecting the lack of macroalgae or other eukaryotic organisms. They form firm to hard surfaces with caramel to greenish color. Detailed examination of these mats reveals three subtypes: *Schizothrix* mats, biofilm mats, and *Solentia* mats, corresponding to Type 1, 2 and 3 mats respectively (Reid et al., 2000).

Schizothrix Mats (Type 1 mat). *Schizothrix* mats are smooth, firm mats consisting of trapped and bound sand grains; macroalgae and other eukaryotes are rare (Fig. 2A,B). They are common on stromatolite surfaces along the reef throughout the year (Table 2). A distinguishing characteristic of this community is the "caramel color" at or near the mat surface (Fig. 2D). The surface itself may have a thin coating of loosely-trapped ooid sand grains (1-2 grains thick) with bare patches exposing the cohesive caramel layer. The caramel layer is typically 0.5 to 1 mm thick and coincides with the highest concentration of oxygen (Fig. 2C,D). The oxygen distribution with depth in the "classic" Type 1 community shows an oxygenated layer that extends ca. 8-10 mm below the surface (Fig. 2C). The broad oxygen maximum (approximately 250% O_2 saturation) suggests that photosynthesis takes place over a wide and diffuse depth interval (Fig. 2C). The blunt shape of the profile and relatively low degree of oxygen saturation compared to other mat systems (e.g., the flat laminated mats of Eleuthera, Bahamas; Dupraz et al., 2004; Braissant et al., 2009) indicates that respiration is also distributed over the top 11 mm and has values that are not very high (Dupraz and Visscher, 2005). This is consistent with earlier observations of *Schizothrix* mats reported by Visscher et al. (1998).

The surface caramel layer consists primarily of *Schizothrix gebeleinii* (Golubic and Brown, 1996, Golubic et al., 2000), a filamentous cyanobacterium that forms a network of single and bundled (two and occasionally three trichomes to a sheath) filaments (Fig. 2E,F)(Stolz et al., 2001). The cells near the surface show faint autofluorescence and are rich in carotenoid, which contributes to the caramel color of the layer. Individual cells in the filament are elongated barrels, 1.5 μm in diameter and from 4 to 8 μm in length (Fig. 2F). The filaments at the surface do not appear to be in any particular orientation (Fig. 2G) as was reported for the *S. gebeleinii* in the stromatolites at Lee Stocking Island (Seong-Joo et al., 2000). *Schizothrix* produces copious quantities of EPS and is an effective trapper and binder of sand grains resulting in the rapid accretion

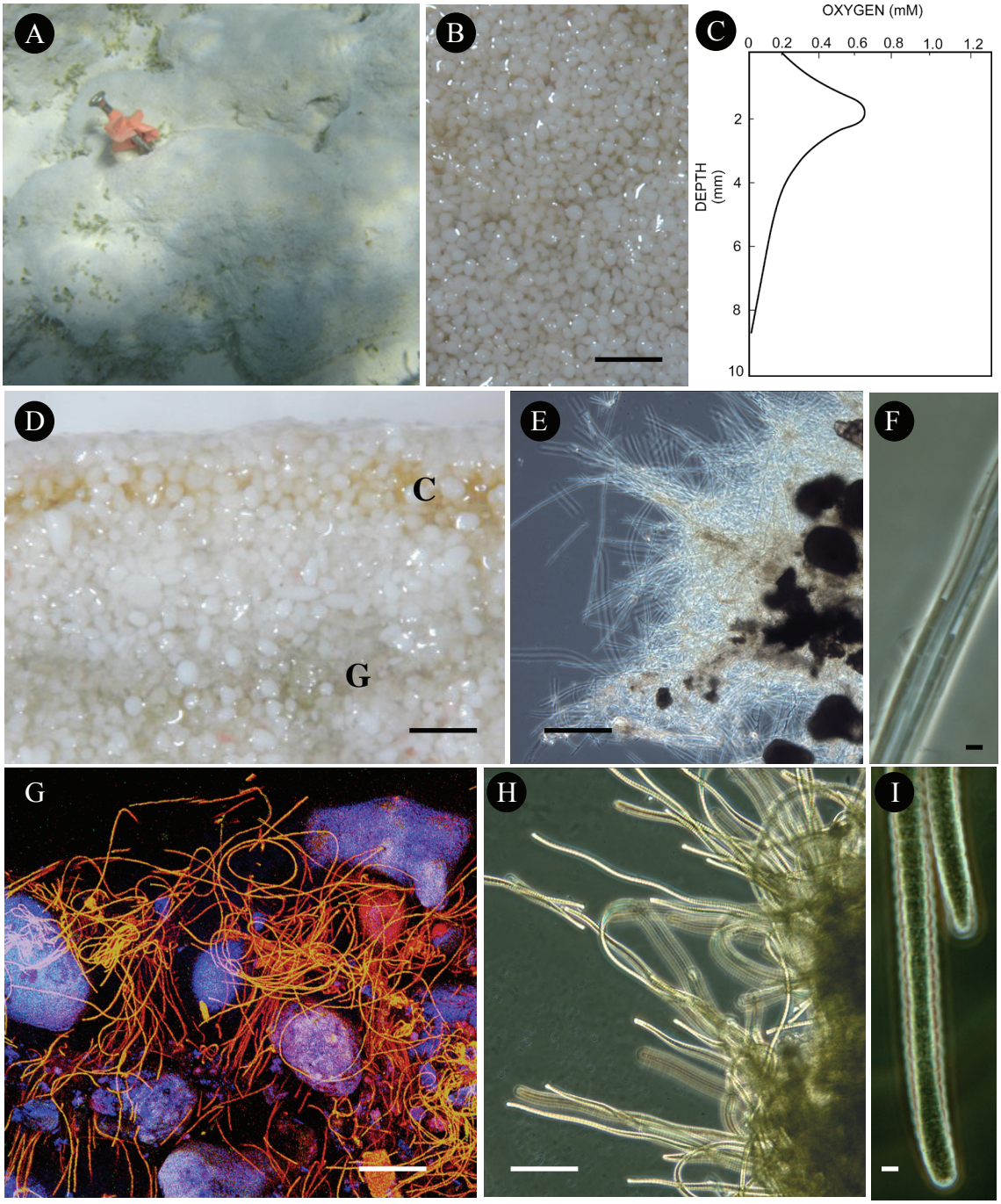

Figure 2. *Schizothrix* mats (Type 1 mat) A) surface as it appears in the field, B) stereomicroscope view of surface, bar 1 mm, C) oxygen profile, D) cross section through top 2.5 mm showing caramel layer (C) and subsurface grey/green (G) layer, bar 0.5 mm, E) *Schizothrix gebeleinii*, PCM, bar is 250 μm, F) close up of *S. gebeleinii* showing multiple filaments in a single sheath, PCM, bar 10 μm, G) surface community visualized by CSLM revealing filaments of *S. gebeleinii* and trapped ooids, bar 150 μm, H) filaments of *Oscillatoria* sp., PCM, bar 25 μm, I) higher magnification of *Oscillatoria* sp. showing rounded terminal cell, PCM, bar 10 μm.

of sediment. Isolated clusters of microcrystalline carbonate (micrite) may be common in the caramel layer. Beneath the caramel layer is a non-pigmented layer that ranges in thickness from <1 mm to several mm (Fig. 2D). The non-pigmented layer is composed primarily of empty sheath material and EPS, as well as single filaments of *Schizothrix*. The filaments exhibit greater fluorescence than the cells in the surface caramel layer indicating more Chl *a*. *Oscillatoria* sp. filaments with disc-shaped cells 6.5 μm in width and between 2.5 and 5 μm in diameter, may also be present in the non-pigmented white layer (Fig. 2H,I). The cells of the *Oscillatoria* sp. are typically light-sensitive, as they readily swell, lyse, and lose their green color (turning a golden color) when illuminated under the light microscope. Further down section, a green-grey pigmented layer may be present (Fig. 2D). This layer is rich in Chl *a*, has abundant single filaments of *Schizothrix* sp., some *Oscillatoria* sp., ooids infested with the boring cyanobacterium, *Solentia* sp., and abundant precipitates. This sub-surface grey-green layer is likely a former *Solentia* mat (i.e., Type 3 mat as described below).

Biofilm Mats (Type 2 mat). The biofilm mat is relatively uncommon, forming only in summer and fall (Table 2). These mats are characterized by a continuous or patchy mucilaginous layer, 20-100 μm thick, which forms on the surface of *Schizothrix* mats. Micritic precipitates are abundant within the biofilm, causing it to appear white. Individual sand grains within or below the white patches are not discernable by eye (Fig. 3A). The thin crusts of micritic precipitate may be soft, with a sugary appearance, or brittle, flaking off when scratched. The oxygen profile in a mat with a surface biofilm over a Type 1 mat is characterized by a shallow oxygen maximum at approximately 1-2 mm below the surface of the mat, with values of 400-600% O_2-saturation (Fig. 3B). The sharp, compact profile and shallow oxygen penetration (ca. 6 mm), result from high rates of photosynthesis, combined with high rates of aerobic and anaerobic respiration (Visscher et al., 1998, 2000; Reid et al., 2000). The biofilms can be difficult to discern from a Type 3 mat in the field but the micritic crusts are clearly evident in cross sections when viewed with a stereo microscope (Fig. 3C). The granular texture of the micritic precipitates is evident in CSLM (Fig. 3D). The biofilm is characterized by rare to absent cyanobacteria. Acridine orange staining (Fig. 3E) and TEM (Stolz et al., 2001, Stolz, 2003) reveal an abundance of small bacteria, 0.25 to 0.5 μm in size. The bacterial population within the biofilm is composed of sulfate reducing bacteria that are actively involved in carbonate precipitation (Visscher et al., 1998, 2000; Baumgartner et al., 2006). The Type 2 mat most often overlays a former Type 1 mat (Fig. 3C), with predominantly single filaments of *S. gebeleinii* that are oriented perpendicular to the surface (Fig. 3D). The filaments, with individual cells 1.5 μm in diameter and 4 to 8 μm in length (Fig. 3F), contain carotenoid but little Chl *a* (Fig. 3G).

*Solentia Mats (Type 3 mat)***.** The *Solentia* mat community is a common mat type that can be found all year but is most abundant in winter and spring (Table 2). The mats form crusty to hard smooth surfaces (Fig. 4A). *Solentia* mats commonly have a well-developed micritic crust (50-100 μm) at the surface, and individual ooids on the mat surface can be difficult to discern due to copious amounts of precipitate (Fig. 4A,C). Macro-algae colonization is sparse, but encrusting and boring organisms are

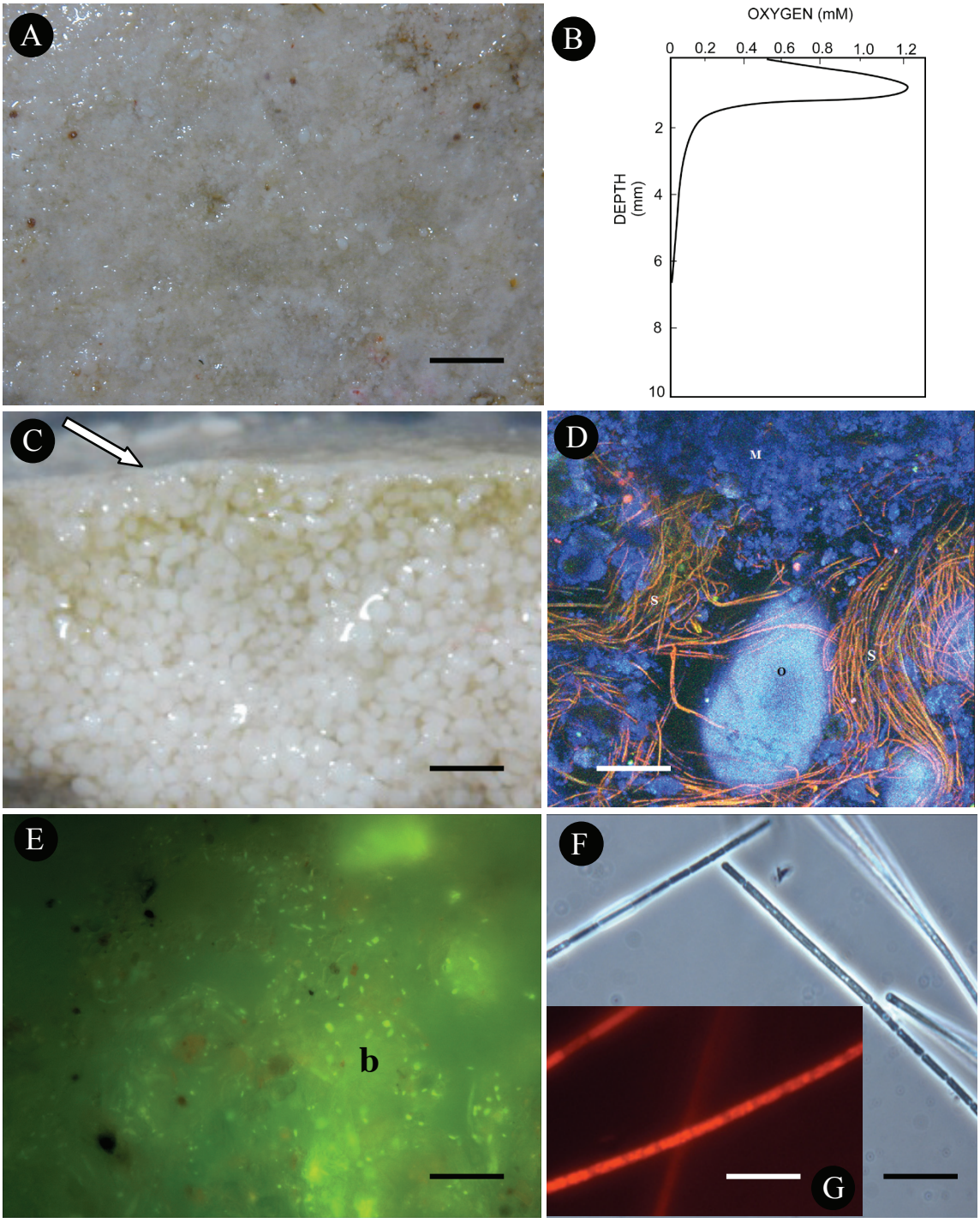

Figure 3. Biofilm mats (Type 2 mat). A) stereoscope view of top surface; note the white surface crust which obscures individual sand grains, bar 1 mm, B) oxygen profile, C) cross section through top 2.5 mm revealing thin micrite layer (arrow), bar 0.5 mm, D) cross section of top 0.5 mm as visualized by CSLM, showing micrite layer (M), large ooid (O), and filaments of *S. gebeleinii* below it (S), bar 50 µm, E) surface biofilm as visualized by FM with bacterial cells stained with acridine orange (bright spots, b), bar 10 µm, F) single filaments of *S. gebeleinii* in caramel layer below the surface biofilm, PCM, G) single filaments of *S. gebeleinii* imaged with FM, bar 10 µm.

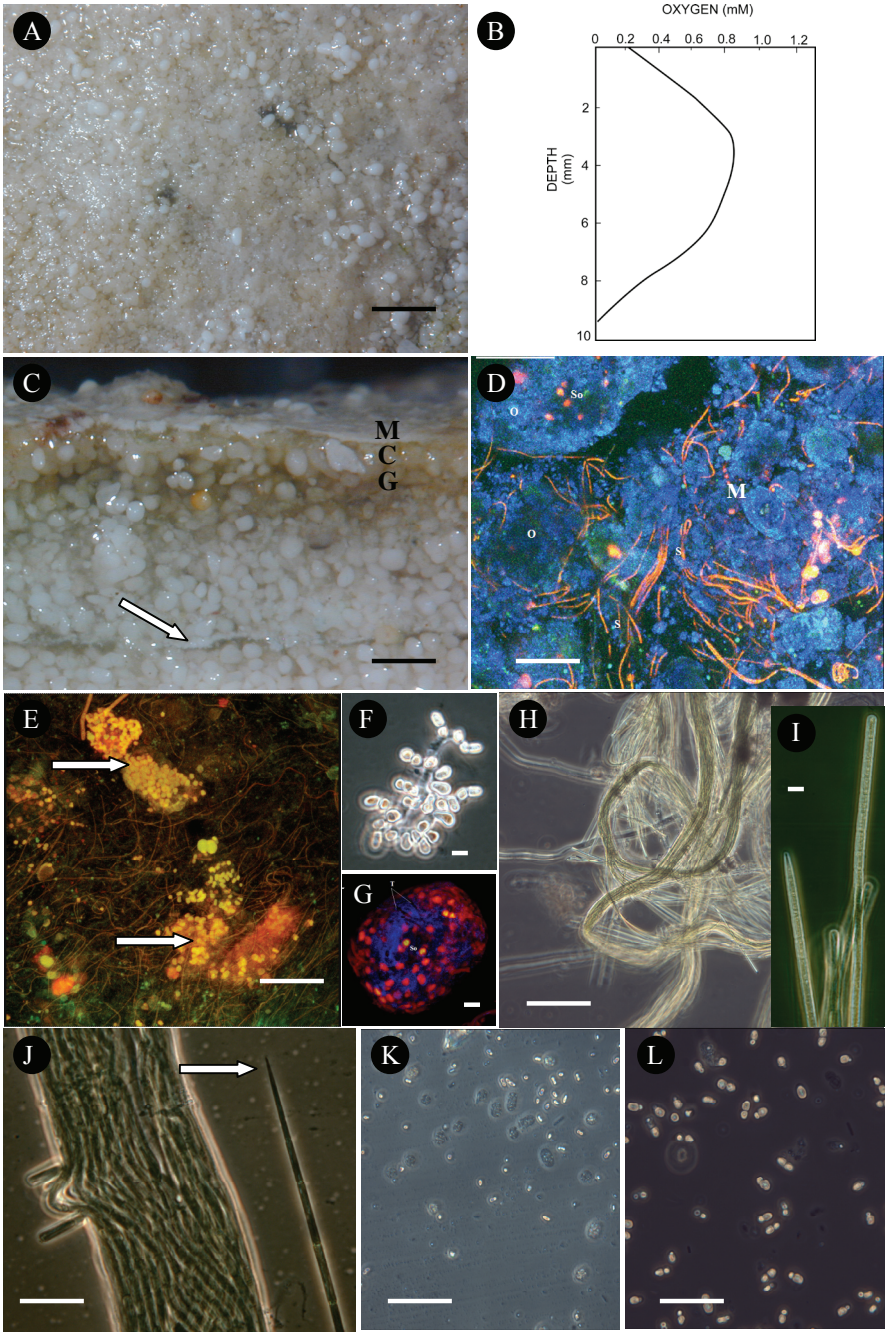

Figure 4. *Solentia* mats (Type 3 mat). A) stereoscope view of top surface; note white surface crust which obscures individual sand grains, bar 1 mm, B) oxygen profile, C) cross section through top 2.5 mm revealing micrite surface layer (M) underlain by a thin caramel layer (C), and a grey/green layer (G), a relic micrite layer at a depth of ~2 mm (a previous surface Type 2 mat) is indicated with an arrow, bar 0.5 mm, D) cross section of top 0.5 mm as visualized by CSLM showing copious carbonate precipitation (M), well bored ooids (O), and filaments of *S. gebeleinii*, bar 10 µm, E) acid-treated surface layer showing filaments of *S. gebeleinii* and clusters of *Solentia* sp. (arrows), bar 100 µm, F) cluster of *Solentia* sp. liberated from an ooid by acid treatment, bar 10 µm, G) *Solentia* sp. infested ooid visualized by CSLM, bar 10 µm, H) bundles of *Microcoleus cthonoplastes*, PCM, bar 10 µm, I) higher magnification of individual cells of *M. chthonoplastes* showing the diagnostic tapered terminal cell, bar 10 µm, J) bundle and single filament of a different species of *Microcoleus* with needle shaped terminal cells (arrow), PCM, bar 10 µm, K) sulfur oxidizing bacteria, PCM, bar 10 µm, and K) unidentified heterotrophic bacterium with distinct (peanut shaped) morphology, PCM, bar 10 µm.

common. Just below the surface lie a caramel and a grey-green layer with abundant flocculent precipitate (Fig. 4C). The oxygen maximum, which occurs below the crust, is very blunt and broad, covering a depth of 5-6 mm (Fig. 4B). The photosynthetic rates are high, resulting in a ca. 300% saturation of O_2. This feature (the blunt and broad profile) is explained by the co-existence of phototrophs and both aerobic and anaerobic heterotrophs. The particular hand sample also shows a micrite layer at about 2 mm depth, indicating a previous Type 2 mat (Fig. 4C). A close examination of the ooids in the subsurface layer reveal that many are infested with coccoid endolithic cyanobacteria that include species of *Solentia* and *Hyella* (Gektidis and Golubic,1996; Al-Thukair and Golubic,1996). These grains show various stages of alteration, often losing their ovoid shape and appearing to "welded together" (Fig. 4D).

The *Solentia* mats are characterized by a diverse microbial community and the highest total biomass of the three "classic" mat types. This suggests that it represents the climax community in stromatolite biogenesis (Reid et al., 2000; Stolz et al., 2001, Stolz, 2003). As in the Type 2 Mats, the thin biofilm and micrite crust at the surface of many Type 3 mats is populated by sulfate reducers. The surface may also be dotted with a common, but as yet unidentified endolithic microalga as well as several species of endolithic cyanobacteria (including *Solentia* and *Hyella* spp.). The grey-green layer, which may lie close to the surface (Fig. 4C) is typically rich in carotenoid and Chl *a* and harbors a diverse community of cyanobacteria. Many of the ooids contain endolithic cyanobacteria (Fig. 4E,F,G) , with varying stages of infestation (Fig. 4E) from a few cells to complete infestation (Fig. 4G). Acid (mild HCl) removal of the carbonate has revealed a variety of morphologies (Fig. 4E,F) suggesting that there could be several different genera. Thus a more detailed investigation to characterize and identify the different morphotypes is warranted. A variety of filamentous cyanobacteria are also present in the grey-green layers, including *Microcoleus chthonoplastes* (Fig. 4H,I), several species of *Oscillatoria*, and an abundance of single filaments of *Schizothrix* (Fig. 4D,E). Occasionally a unique species of *Microcoleus* that forms thick bundles with 10-20 trichomes was observed. Similar to *M. chthonoplastes*, the cells in the trichome are barrel shaped, 5 x 10 μm, but the terminal cells taper to a needle point (Fig. 4J). Other non-photosynthetic but morphologically distinct bacteria were also been seen in abundance including colorless sulfur-oxidizing bacteria (Fig. 4K) and a large motile dumbbell-shaped bacterium (Fig. 4L).

Stalked Diatom Mats

The stalked diatom surface mats are abundant along the reef in summer and fall but sparse in the winter and spring (Table 2). They are easily identifiable in the field as pink "fuzz" (<0.5 cm in thickness), yellow "fuzz" (<0.5 cm in thickness), or a conspicuous yellow "fur" (1-2 cm in thickness) covering firm mat surfaces (Fig. 5A,B). Although the diatoms contain chlorophyll and are presumed to be obligate oxygenic phototrophs, the oxygen they produce quickly diffuses into the water column (Fig. 5C). A typical profile has a relatively sharp maximum of ca. 400% saturation at 2 mm depth and anoxia at 8 mm depth (Fig. 5C). The oxygen peak coincides with the caramel layer and similar to the *Schizothrix* mats, is indicative of a relatively low abundance of aerobic

heterotrophs and low rates of respiration. Thus the subsurface microbial community is the dominant feature of the oxygen profile of the stalked diatom mat.

The stalked diatom communities commonly baffle sediment and accumulate loosely trapped grains up to several millimeters thick; 3-5 mm in pink or yellow fuzz and to 1-2 cm in yellow fur (Fig. 5D). The pink fuzz is comprised primarily of the stalked diatom *Striatella unipunctata* (Lyngbye) Agardh (Fig. 5E,F). The cells are square, 75 μm by 80 μm, to rectangular with the stalk attached to a corner (Fig. 5F). The stalk is 5 μm in diameter, but may be over hundreds of μms in length. The yellow fuzz is formed by an association between the stalked diatom *Licmophora remulus* Grunow and a species of *Oscillatoria* (Fig. 5G). The filaments of *Oscillatoria* sp. are 12 μm in diameter and 100's of microns in length and produce a thin sheath (Fig. 5H). Individual filaments may stick straight out from the stromatolite surface into the water column. The cells of *L. remulus*, which are usually 10 μm at their greatest diameter and up to 75 μm in length, attach to the sheath of the *Oscillatoria* sp. initially by a holdfast region at the base of the diatom (Fig. 5G, Franks et al., 2009). This holdfast may develop further into a stalk as the density of the diatom population increases. In addition to *L. remulus* a well-developed yellow fur may consist of a number of additional diatom species including a larger species of *Licmophora, L. paradoxa* (Lyngbye) Agardh, with cells of the dimensions of 20 μm x 150 μm (Fig. 5I), as well as *S. unipunctata* and the chain-forming diatom *Thalassionema* sp..

The stalks of dense yellow fur typically occur in bundles, forming discrete vertical "gelatinous channels" in the subsurface (Fig. 5D). These trunks extend below the firm mat surface providing evidence that the mat has accreted upward, burying the older bundled stalks (Franks et al., 2009). Strong wind events erode the diatoms and the loosely bound surface sediment trapped by the fur and fuzz. This exposes the underlying firm caramel layer of filamentous cyanobacteria. Surfaces that have been stripped clean of the yellow fur appear to have green dots on their surface (Fig. 5B). These "gel dots" are actually the tops of subsurface gelatinous channels (Franks et al., 2009). The channels often become colonized by a species of *Oscillatoria* suggesting that the remnant diatom stalks may actually conduct light deeper into the subsurface (Franks et al., 2009).

Tube Diatom Mats

Tube diatom mats are abundant on stromatolite surfaces along the reef in fall and winter. These mats become rare in spring, gradually appearing again in late summer (Table 2). Two distinct, seasonal morphologies are observed. In the summer and fall, the tube diatom mats form as discrete pustules, up to 5 cm in diameter, on the top surfaces of stromatolites (Fig. 6A). Composed of loosely consolidated grains, the pustules display a stringy texture when disturbed (Fig. 6C). In winter and spring, stalked diatom pustules coalesce into a blanket covering the stromatolite surface (Fig. 6B). This blanket has a distinct meringue-like surface texture (Fig. 6D). Blankets of loosely bound sediment up to 1 cm thick can form within a matter of days. Like the stalked diatom mats, tube diatom mats are eroded during heavy winds, exposing the underlying firm surface, which is

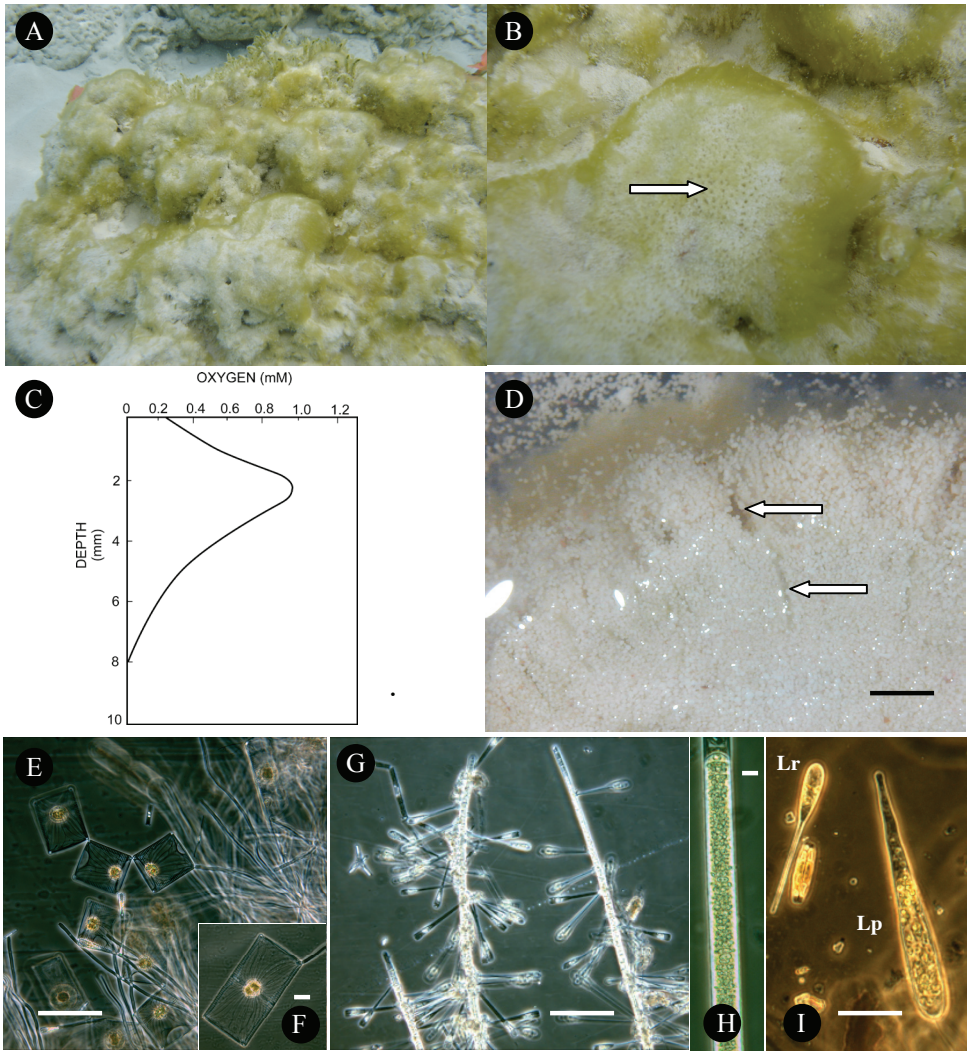

Figure 5. Stalked diatom mats. A) field view of stromatolite surface covered with yellow fuzz and patches of yellow fur. B) surface of yellow fur that had been recently eroded to reveal the "gel dots" (arrow), C) oxygen profile, D) cross section through the top 5 mm of a yellow fur showing loosely bound ooids near the surface and vertical gelatinous channels (arrows), bar 1 mm, E) mass of *Striatella unipunctata*, PCM, bar 100 µm, F) higher magnification of an individual cell of *S. unipunctata* with attached stalk, PCM, bar 20 µm G) cells of *Licmorpha rimulus* attached to a filament of *Oscillatoria* sp., PCM, bar 50 µm. H) *Oscillatoria* sp., PCM, bar 10 µm, I) cells of *Licmorpha rimulus* (Lr) and *Licmorpha paradoxa* (Lp) from yellow fur, PCM, bar 50 µm.

typically a Type 1 mat. The pustular blanket supports little oxygen production (Fig. 6E) The oxygenated zone only extends to 6-8 mm depth and the maximum value for oxygen is less than 150% saturation. This suggests low cyanobacterial abundance as well as low activities of aerobic heterotrophic bacteria.

Microscopic examination of the stringy pustules and pustular blanket reveal they consist of a diatom that forms unique sheaths of EPS (Fig. 6F,G). Several genera of diatoms are known to produce tubular EPS including species of *Nitzschia*, *Navicula*, and *Amphipleura rutilans* (S. Golubic, pers. comm.). Although not heavily pigmented, they do contain chloroplasts with Chl *a* as is evident from the CSLM and PCM images

(Figs. 6F,G). The tubular EPS is ~ 8-10 µm in width. The diatoms are approximately 5 µm in with and 15 µm in length, suggestive of Naviculid species. The cells form long chains within the sheath (Fig. 6G) and are very motile and extremely light sensitive. When exposed to light (e.g., under the light microscope) they readily evacuate their tubes of EPS, leaving behind little evidence of their presence. Interestingly, the tube diatom EPS is different in composition than that produced by the stalked diatoms (Franks et

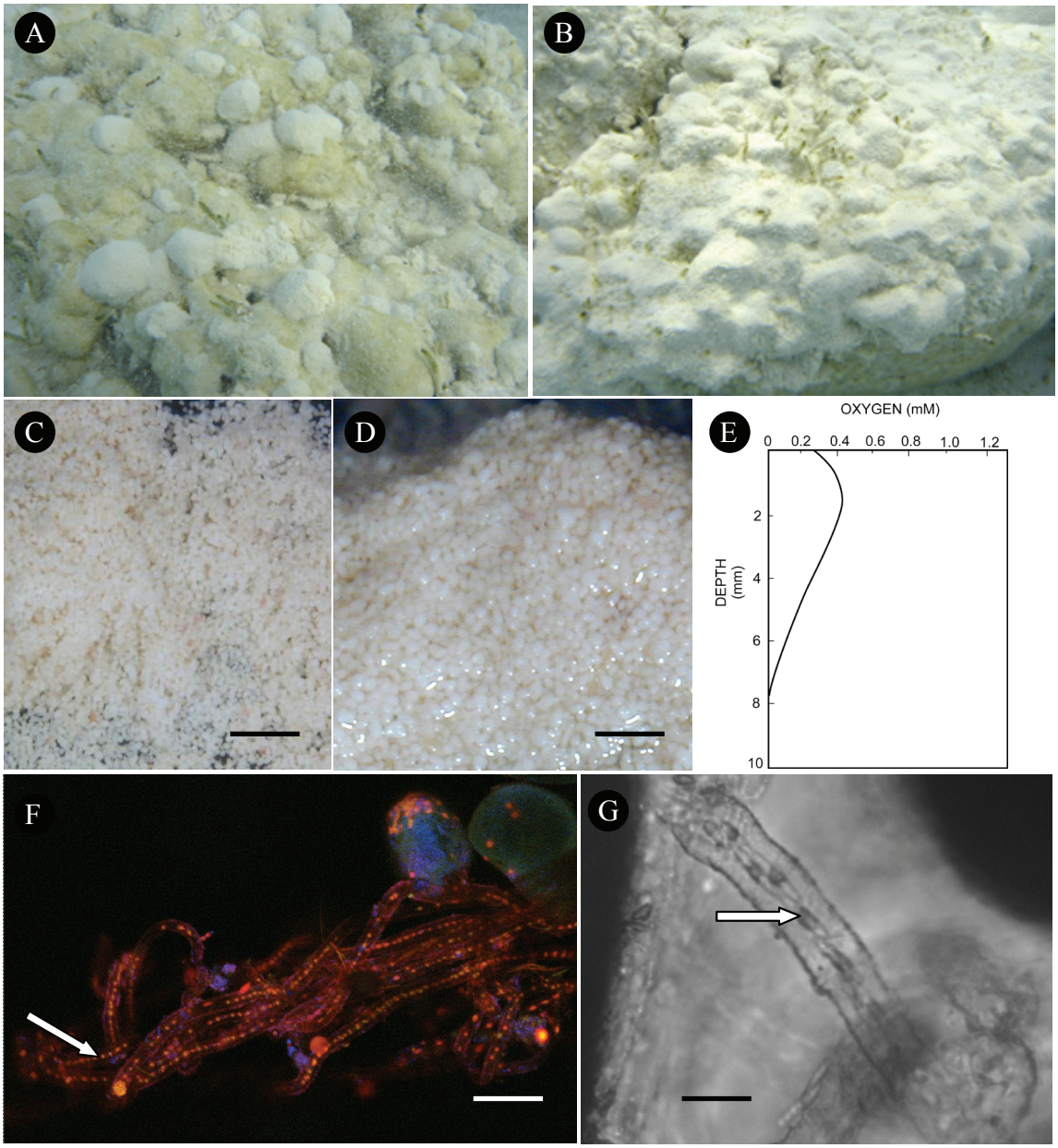

Figure 6. Tube diatom mats. Field view of A) stringy pustules and B) pustular blanket. Stereoscope view of a stringy pustule C), and pustular blanket D) revealing cohesiveness of the sample but lack of mat forming cyanobacteria or stalked diatoms, E) oxygen profile of pustular blanket, F) tube diatoms from stringy pustule as visualized by CSCM indicating cells possess chloroplasts with Chl *a* (arrow), bar 100 µm, G) higher magnification of tubes from stringy pustule revealing Naviculid-like diatoms in sheath, chloroplasts are visible within the individual cells. (arrow), PCM, bar 10 µm.

al., 2009). Nevertheless, it does show a propensity to trap ooids (Fig. 6C). Carbonate precipitates are also abundant in these mats (Franks et al., 2009), but whether the diatoms themselves directly are involved in the precipitation is not known.

Pudding Mats

Pudding mats are small, cohesive mounds of loosely bound grains on the top surfaces of stromatolites (Fig. 7A). They are common during the summer, rare in spring and fall, and not present in winter (Table 2). These mounds, which are 2-12 cm in diameter and resemble dollops of pudding, commonly envelop *Batophora* stalks (Fig. 7A). Although the oxygen profile of an individual pudding mat may vary depending on the oxygenic phototrophs present (see below), it has the general characteristics of those seen in Type 1 mats (Fig. 7B). The oxygen distribution is diffuse with the maximum O_2 concentration reaching ca. 200 - 250% saturation and the oxic zone of the mat extending to a considerable depth (up to 24 mm). The profile shows a sharp increase in oxygen at a depth of 1.5 - 2 mm, which may be due to the presence of a population of single filament *Schizothrix*. The lack of significant heterotrophic consumption (also typical for the Type 1 community) allows the oxygen to penetrate to greater depth.

Several different forms of pudding mats have been recognized based on their relative cohesiveness and color. Soft pudding is non-pigmented and gives with slight pressure while firm puddings have a caramel colored surface (Fig. 7C) and can withstand slight pressure. Soft puddings form on the tops of stromatolites and become more cohesive in the course of a weeks resulting in firm mats, suggesting an ecological succession of different microbial populations. Light microscopy of acid treated samples (where the ooids were dissolved away improving the resolution of the microscopy) revealed that the pudding mats are composed mainly of a very thin sheathed filamentous cyanobacterium, 0.25 μm in diameter (Fig. 7E). Its very thin diameter makes it difficult to identify under normal fluorescence and CSLM imaging as it only faintly autofluoresces. We have tentatively identified it as a species of *Phormidium*. The organism forms a network of filaments that trap the ooids. This network becomes infiltrated with single filaments of *S. gebelineii* (Fig. 7E) which eventually becomes the dominate organism (imparting the caramel color), in the progression from soft to firm pudding.

A variant of the firm pudding, called “coccoid pudding”, has a dark green layer of coccoid cyanobacteria at a depth of 1-3 mm (Fig. 7D). Pudding with this layer of cyanobacteria can be recognized from the accumulation of oxygen bubbles at the surface. We have tentatively identified the coccoid as a species of *Cyanothece* (J. Waterbury, pers. comm.). The cells show intense fluorescence indicating a high concentration of chlorophyll a (Fig. 7F). Under phase contrast microscopy, the cells have a highly refractive cell wall and a conspicuous intracellular inclusion that extends down the center axis of the cell (Fig. 7G). The ultrastructure shows features common for cyanobacteria including thylakoids, carboxysomes, cyanophycin granules and a Gram negative cell wall (Fig. 7H). The emission spectrum generated from the CSLM also indicates the presence of phycobilin pigments. Despite the highly compartmentalized cytoplasm, the cells divide by binary fission with cells ranging in size from 5 to 10 μm in diameter.

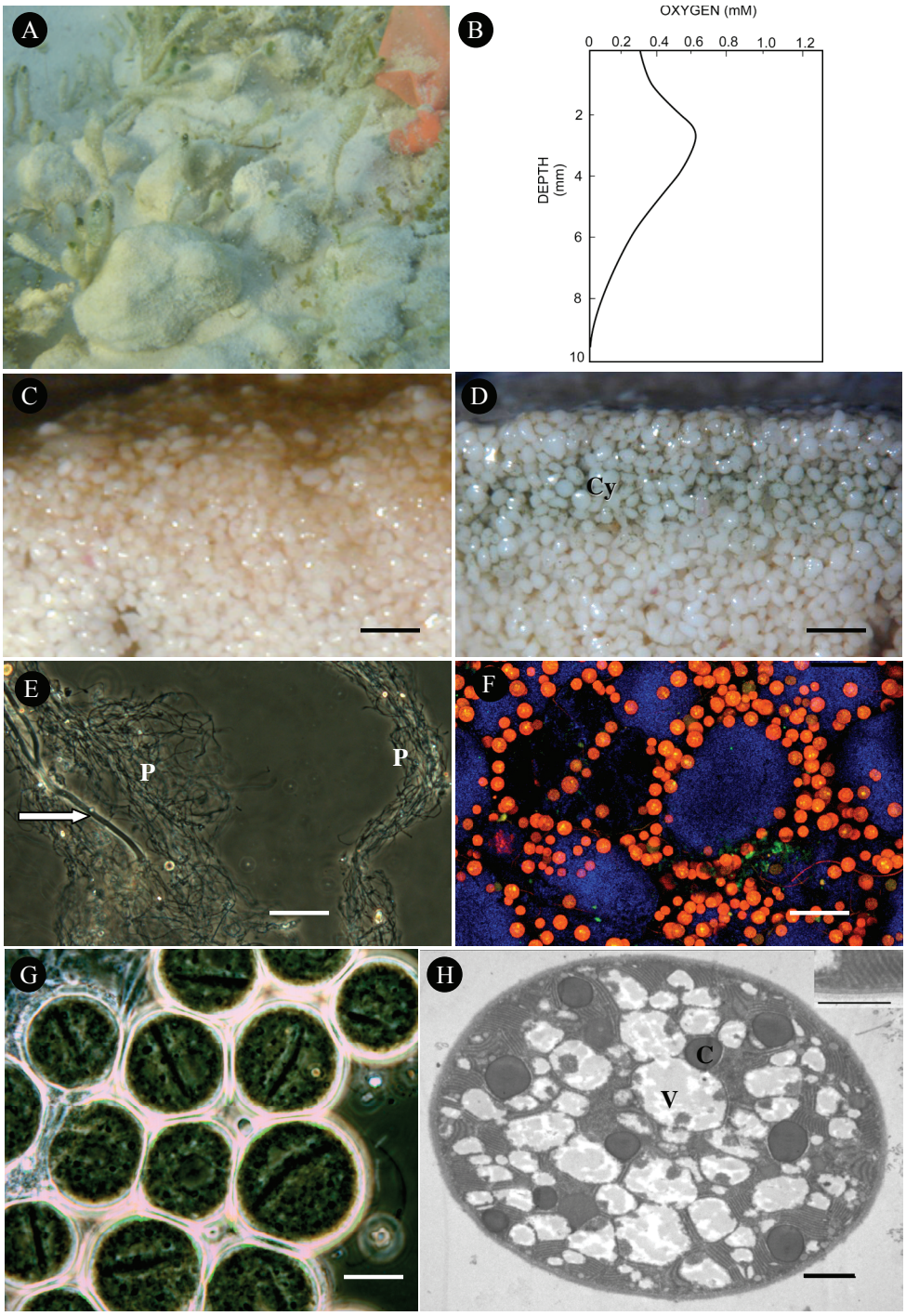

Figure 7. Pudding mats. A) surface as it appears in the field showing close association with thalli of *Batophora* sp., B) oxygen profile, C) cross section through top 3 mm of a firm pudding with caramel pigment, bar 1 mm, D) cross section through top 4 mm of a coccoid pudding with a layer of *Cyanothece* sp. (Cy), bar 1 mm, E) filaments of *Phormidium* sp. (P) and *S. gebeleinii* (arrow) from the caramel surface of firm pudding after the ooids have been removed by acid treatment, PCM, bar 15 µm, F) higher magnification of the *Cyanothece* sp. dominated layer of a coccoid pudding as imaged by CSLM, bar 50 µm, G) individual cells of *Cyanothece* sp. as imaged by PCM showing range of diameters and distinctive bar-shaped intracellular inclusion, H) ultrastructure of *Cyanothece* sp. revealing vacuolated cytoplasm (V), intracellular inclusions (cyanophycin, (C)) and thylakoids, bar 1 µm, insert shows details of Gram negative wall and thylakoid structure, bar 500 nm.

Community Fingerprinting

A preliminary assessment of species diversity in the different mat types by molecular approaches was done using DGGE (Fig. 8). The results provide a fingerprint for the microbial communities in the following mat types. For the "Classic" mats, Type 1 (*Schizothrix*) mats and Type 2 (biofilm) mats were analyzed. For the stalked diatom mats yellow fur and pink fuzz were analyzed. For the tube diatom mats stringy pustule and pustular blanket were analyzed. For the pudding mats soft, coccoid and firm puddings were analyzed. Each mat type contained between 40-60 distinct bands suggesting that the mats have high species richness (Fig. 8). Cluster analysis of the DGGE fingerprints revealed the mat types group into two major clades. The top clade contains "Classic" Type 1 and Type 2 mats and both yellow fur and pink fuzz of the stalked diatom mats. The lower clade contains the tube diatom mats (stringy pustule and pustular blanket) and all three pudding mats (smooth, firm, and coccoid). Within the two major clades, four distinct clusters are observed. Cluster I contains the stalked diatom mats (yellow fur and pink fuzz) and Type 1 mats. Cluster II contains only the Type 2 mats. Cluster III contains only the tube diatom mats, while Cluster IV contains all pudding mats. These results suggest that the microbial composition of the "classic" mats and stalked diatom mats have more in common and that the tube diatom mats and pudding mats are unique. They also support the designation of the four major mat types that was based on morphology, color, hardness, and dominant organisms. A clearer picture will emerge once more detailed molecular analyses become available.

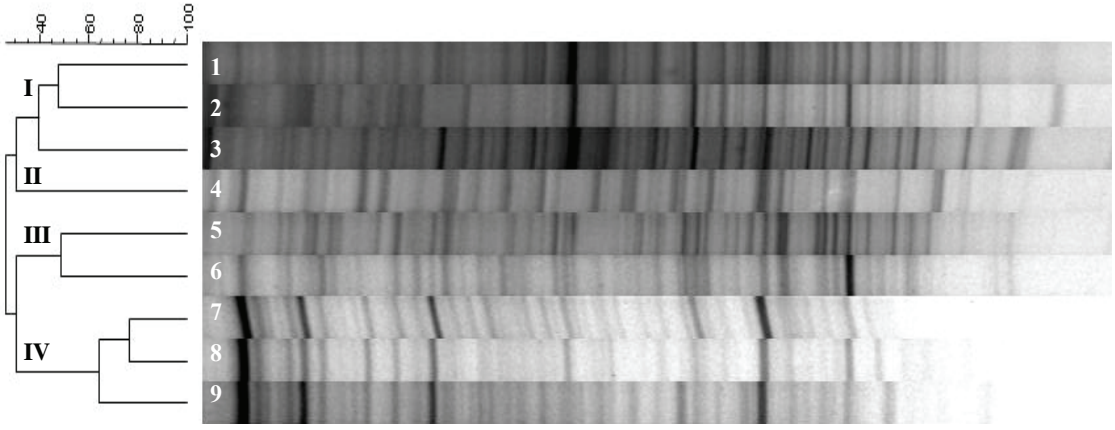

Figure 8. Cluster analysis of bacterial communities found in different stromatolite mat types. Right side of figure is a negative image of the bacterial 16S rRNA gene fragments separated by DGGE from mat types. Lanes represent: 1) yellow fur, 2) pink fuzz, 3) Type 1 mat, 4) Type 2 mat, 5) stringy pustule, 6) pustular blanket, 7) soft pudding, 8) coccoid pudding, and 9) firm pudding. Left side of figure is a similarity dendrogram after UPGMA-computation by Dice's coefficient. The small numbers at each node are the cophenetic correlations and the roman numerals (I-IV) mark the four distinct clusters. The scale bar represents the percent similarity.

Carbohydrate Fractions in the Different Mat Types

The results of carbohydrate extractions for the following mat types are summarized in Table 3. For the "classic" mats, types 1 and 2 mats were combined and the top 3 mm analyzed. Type 3 mats (the top 3 mm) were analyzed separately. For the stalked diatom mats, yellow fur was subdivided into upper (the upper millimeter of firm mat plus overlying diatoms and loosely bound sediment) and lower (1-4 mm depth within firm mat). For pudding mats, coccoid puddings were used and subdivided into upper (top 1 mm) and lower (1-3 mm depth). The different mat types show distinct variations in overall abundance of carbohydrate and in the relative amounts in each of the various extracts.

Table 3. Results of carbohydrate and Chl *a* extractions for different stromatolite mat types: (1) *Schizothrix* and Biofilm mats (Type 1 and Type 2*)*, (2) *Solentia* mats (Type 3); (3) Stalked diatom Yellow Fur (tubes and upper mm of firm mat) and underlying mat; and (4) Coccoid pudding mat (upper mm containing coccoids, and lower layers). Carbohydrate extracts are colloidal low-molecular weight fraction carbohydrate (cLMW); colloidal EPS (cEPS); hot-water carbohydrate (HW); hot bicarbonate low molecular weight carbohydrate (HB-LMW); and hot bicarbonate EPS (HB-EPS). Concentrations of carbohydrate are presented as mean ± SD expressed as µg glucose equivalents cm^{-2} mm^{-1} of mat, and as a % of the total extracted carbohydrate (in parentheses). Total is the sum of the extracted carbohydrate fractions. Chl *a* µg cm^{-2} mm^{-1}, N= number of samples.

MAT-TYPE	*N*	*cLMW*	*cEPS*	*HW*	*HB-LMW*	*HB-EPS*	*Total*	*Chl* a
Types 1 and 2	6	16 ± 2 (8.3%)	17 ± 3 (8.9%)	19 ± 1 (9.9)	9 ± 1 (4.7%)	131 ± 27 (68.2%)	192	3.5 ± 0.5
Type 3	4	35 ± 8 (10.7%)	54 ± 9 (16.7%)	33 ± 3 (10.1)	10 ± 2 (3.1%)	194 ± 48 (59.5%)	326	2.9 ± 0.4
Stalked diatom, top (stalks & 0-1 mm firm mat)	5	30 ± 2 (14.0%)	37 ± 2 (17.3%)	71 ±6 (33.2)	4 ± 1 (1.9%)	72 ±7 (33.6%)	214	0.3 ± 0.04
Stalked diatom, lower (1-5 mm within firm mat)	5	7 ± 1 (5.3%)	21 ± 4 (15.8%)	56 ± 5 (42.1%)	5 ± 1 (3.8%)	44 ± 6 (33.1%)	133	0.6 ± 0.1
Coccoid Pudding (0-1 mm)	5	70 ±3 (34.3%)	19 ± 6 (9.3%)	34 ±12 (16.7%)	7 ±1 (3.4)	74 ± 9 (36.3%)	204	2.2 ± 0.2
Coccoid Pudding (1-3 mm)	5	11 ±2 (9.9%)	5 ± 1 (4.5%)	30 ± 4 (27.0%)	3 ±1 (2.7)	62 ± 6 (55.9%)	111	0.4 ± 0.1
ooids	3	1 ± 0.1 (9.1%)	1 ± 0.2 (9.1%)	3 ± 0.2 (27.2%)	2 ± 0.4 (18.2)	4 ± 0.2 (36.4%)	11	

Schizothrix and Biofilm Mats (Type 1 and Type 2 mats). These mats had the highest Chl *a* concentrations, and carbohydrate is dominated by structural EPS in the HB-EPS fraction (131 ± 27 µg, 68.2 % of the total). Colloidal carbohydrate is generally low, with approximately equal amounts of cLMW (16 ± 2 µg) and cEPS (17 ± 3 µg).

Solentia Mats (Type 3 mats). The highest carbohydrate concentrations of all the mats measured occurred in the *Solentia* mats. This was predominantly due to high HB-EPS (194 ± 48 µg, 59.5% of total), but there was also high concentrations of colloidal

carbohydrates (cLMW and cEPS). In the *Solentia* mats, there were proportionally more cEPS (54 ± 9 μg) relative to cLMW (35 ± 8 μg) than the Type 1 and Type 2 mats, in which the colloidal fractions were approximately equal.

Stalked Diatom (Yellow fur mats). Despite low Chl *a* concentrations, the upper mm of yellow fur mats show relatively high proportions of colloidal carbohydrates (31.3% of the total carbohydrate extracted), with cLMW (30 ±2 μg) almost equal to cEPS concentrations 37 ±3 μg. The concentrations, and proportions of HW carbohydrate were much higher than in *Schizothrix*, Biofilm, and *Solentia* mats. The lower mat section had double the Chl *a* concentration as the upper layer, but less carbohydrate in all fractions, and proportionally less cLMW (7 ± 1 μg) relative to cEPS (21 ± 4 μg), and less HB-EPS (44 ± 6 μg) than in the upper mat. Compared to the cyanobacteria-dominated mat types (1, 2 and 3), HB-EPS was proportionally less abundant in the yellow fur mats.

Pudding Mats. Lower overall concentrations of carbohydrate were measured in coccoid pudding mats compared to Type 1, 2 and 3 mats. However, the upper mm of the pudding mats, containing the green coccoids, showed the highest concentrations and proportions of cLMW (34.3% of total) of all mat types (corresponding with high Chl *a* concentrations), with cEPS only about 20% of the colloidal extract. This is lower than any of the other mat types studied (Table 3). The lower section of the pudding mats contained very little cEPS or cLMW, and low amounts of HW and HB extracts. The major constituent of EPS in the lower section of the pudding mats was HB-EPS (62 ± 6 μg, 55.9 % of total extracted carbohydrate).

Ooid sand. The ooid sand contained almost no carbohydrate in any of the extracts.

DISCUSSION

Microbial Community Composition

Stromatolites have been found in a number of locations on the margins of Exuma Sound, including Schooner Cays, near Eleuthera (Dravis, 1983); Adderly Cut, north of Lee Stocking Island (Dill et al., 1986) and througout the Exuma Cays (Reid et al., 1995). They range in distribution from intertidal to subtidal and differ in microbial community composition (Seong-Joo et al., 2000). The extensive monitoring program at Highborne Cay undertaken by the RIBS team has resulted in the realization that stromatolites are very dynamic systems that exhibit heterogeneity on both spatial and temporal scales (Perkins et al., 2007; Eckman et al., 2008; Paterson et al., 2008). The surface microbial mat communities at Highborne Cay have been categorized into four major groups based on morphology, color, hardness, and dominant organisms: “Classic mats” (*Schizothrix* mat, Biofilm mat, *Solentia* mat), stalked diatom mats, tube diatom mats, and puddings (Table 1). Each of the mat types had a unique oxygen profile that reflected both the presence of oxygenic phototrophs (e.g., cyanobacteria, diatoms) as well

as aerobic respiring heterotrophic organisms, and presumably distinct biogeochemical processes. The designation of the four major mat communities was further supported by molecular finger printing DGGE analyses (Fig. 8). More importantly, the relative abundance of each mat type appears to be seasonal, with the *Schizothrix* mat ("Classic" Type 1) being common through out the year. Interestingly, surface mats dominated by diatoms were most prevalent during the late summer months. Thus one can easily get a different impression on who the major contributors are in the biogenesis of the bioherms depending on the time of year the sampling is done. The presence of a microbial mat on a stromatolite surface does not, de facto, indicate the role of the mat in subsurface stromatolite accretion. Although stalked diatom, tube diatom and pudding mats are involved in rapid accumulation of loosely bound sediment they are easily eroded. This is due to their susceptibility to burial (Perkins et al., 2008) and the lack of structural EPS (see discussion below). Accretion studies, which will be reported in a separate publication, were conducted in parallel with mat type observations, to ascertain the geologic significance of each mat type. Results from the accretion studies indicate that stabilization of the unconsolidated sediment accreted by diatom and pudding mats ultimately requires binding by *S. gebeleinii* (Bowlin and Reid, pers. comm.).

Differences in the microbial composition of the surface mats were evident through microscopy (e.g., light, fluorescence, CSLM, TEM) as many of the abundant microorganisms had distinct morphologies. Although some organisms could be identified to the species level (e.g., *Schizothrix gebelineii*, *Microcoleus chthonoplastes*, *Licmophora remulus, L. paradoxa Striatella unipunctata*), many could only be identified down to genus (e.g., *Oscillatoria* sp., *Phormidium* sp.). Several are new to science, such as the cyanobacterium in the coccoid pudding, and will need further study. Nevertheless, specific organisms could be linked to specific sedimentary features (e.g., smooth mat, stringy pustules, pudding).

Initial molecular studies are generating lists of microbial species. In one study, 18 different phyla were found in a Type 2 mat including *Proteobacteria*, *Cyanobacteria*, *Firmicutes*, *Planctomycetes*, and *Chloroflexi* (Havemann and Foster, 2008). A subsequent study expanded the total number of sequences to 33 phylotypes (Foster et al., 2009). It is interesting to note that a few of the cyanobacteria identified in the Highborne Cay system have also been found at Shark Bay Australia such as *Microcoleus* and *Cyanothece* (Burns et al., 2004, Goh et al., 2008). However, no *Schizothrix* sequences have yet been found suggesting either a failure to amplify the signal (e.g., poor DNA extraction or cloning bias) or that *S. gebelineii* is a unique species of *Schizothrix*. The results of a molecular survey of viral species present in the stromatolites and thrombolites at Highborne Cay found more than 97% of the viral sequences retrieved were novel (Desnues et al., 2008). They included a large percentage of single-stranded DNA microphages not found in any of the other environments examined (e.g., sea water, fresh water, sediment, terrestrial, extreme, metazoan-associated and marine microbial mats) suggesting these stromatolites harbor a unique viral biota (Desnues et al., 2008). Attempts at obtaining the major mat organisms in pure culture have also met with some success (Havemann and Foster, 2008; Foster et al., 2009). Of the cultivated cyanobacteria from the Type 2 mats 30% have correlated directly to the 16S rRNA gene clone libraries generated from natural

stromatolite samples (Foster et al., 2009). Similar levels of clone and culture library overlap have been reported for other mat systems (e.g., López-Córtez et al., 2001). A combination of more affective DNA extraction, and *in situ* hybridization experiments, in concert with culturing, will be needed to link specific cell morphologies with molecular sequences. Nevertheless, the microbial diversity in the Highborne Cay mat communities is on a par other mat systems (Foster and Green, 2009) such as intertidal mats (Rothrock and García-Pichel, 2005), and the flat laminated mats found in Eleuthera (Baumgartner et al., 2006, 2009), but less than Guerrero Negro, Baja California Mexico (Ley et al., 2006).

Carbohydrate Composition

The concentration of carbohydrates in general, and of the EPS fractions in particular, found in the stromatolite mat communities are higher than those reported for other tropical sediment biofilms. For example Underwood (2002) reported cEPS concentrations of between 5.96 and 18.8 μg cm^{-2} mm^{-1} for a range of intertidal silty and sandy sites in Fiji. Lower cEPS concentrations (1.6 – 6.89 μg cm^{-2} mm^{-1}) have been measured in subtidal biofilms growing on coral sand at Heron Island, Gt. Barrier reef (Underwood, unpublished data). The high carbohydrate concentrations in the stromatolite mats are notable because they indicate the degree of bio-concentration of organic matter in the stromatolites. cEPS and HB-EPS will add structural integrity to the ooid – cyanobacterial filament matrix, which will increase sediment stability in the high energy, wave-washed and physically challenging environment.

Variability in the amounts of carbohydrate in each of the extracts is consistent with the taxonomic composition of the different mats. Colloidal low molecular weight carbohydrate (cLMW) is an indicator of active photosynthesis (Smith and Underwood, 1998; Perkins et al., 2001; Underwood, 2001) and compositional studies on diatom-rich biofilms have found this fraction contains a high proportion of glucose (Bellinger et al., 2005). Concentrations of cLMW carbohydrate change rapidly in biofilms, increasing during periods of photosynthesis and declining rapidly in darkness, due to consumption by heterotrophic action (Hanlon et al., 2006; Haynes et al., 2007). The highest values of cLMW occurred in the chlorophyll *a* – rich upper mm of the cocoid pudding (70 $\pm$3 μg), where photosynthesis by coccoid cyanobacteria generates oxygen bubbles in mid afternoon. cLMW was also high in the upper portions of the stalked diatom yellow fur mats, where substantial number of viable diatoms and cyanobacterial filaments were found. These data suggest that these regions of both mat types were areas of active photosynthesis.

In intertidal diatom-dominated sediments cEPS is often about 25% of the colloidal carbohydrate fraction. In the stromatolite mats, cEPS was often > 50% of the colloidal carbohydrate. By definition, this fraction is polymeric and has potential structural properties (Decho, 2000). There may be a selective pressure to produce more cEPS to maintain the structure of the mats. cEPS can be produced both during photosynthesis and in the absence of light, using intracellular carbohydrate storage compounds (Underwood et al., 2004). Proportionally, cEPS was highest in Type 3 mat (54 $\pm$ 9 μg), with abundant *Solentia* – and in the upper portion of the yellow fur-stalked diatom mats. It is known

that benthic diatoms produce large quantities of cEPS (Underwood and Paterson, 2003), whether the high proportions in Type 3 mats represent cEPS production by *Solentia*, or by other cyanobacteria in these mats remains to be determined.

The hot-water extractable carbohydrate fraction of mats (HW) has been shown to contain β1-3 linked glucans, the storage product of diatoms, and correlate closely with benthic diatom biomass (Chiovitti et al., 2004;Bellinger et al., 2005; Abdullahi et al.; 2006). It is likely that hot-water treatment will also extract carbohydrate from cyanobacteria though it is not know if this is intracellular or extracellular. The highest concentrations of HW occurred in the diatom-rich upper yellow-fur mat samples (71 ± 6 μg) and yellow fur lower, which still had diatom stalks (56 ± 5 μg). This was despite low concentrations of Chl *a* in these mats, compared to the phototrophic biomass present on the cyanobacteria-dominated mats (e.g. Type 1, 2 and 3 mats). This indicates a stronger relationship between diatom biomass and HW-extracted carbohydrates than between cyanobacteria and HW.

The hot bicarbonate extraction solubilizes EPS that is tightly bound or cross-linked (Wustman et al., 1998; Abdullahi et al., 2006). Though there is a small amount of HB-LMW present in the hot bicarbonate extracts, the majority of material obtained is polymeric (ie HB-EPS). The hot bicarbonate extract is therefore mainly highly structural EPS, containing the stalks of the diatoms and cyanobacteria sheaths. The greatest concentrations of HB-EPS occurred in the "classic" mat types corresponding to the high photoautotrophic biomass of cyanobacteria in these mats. The other mat types had lower amounts of HB-EPS. Though the diatom stalks consisted primarily of HB-soluble EPS (they were completed dissolved by the HB extractions), and stalks contributed a greater proportion of the total carbohydrate in the upper layers, the actual biomass present, despite their high visual impact, was relatively low in comparison with the cyanobacteria-rich mats. High concentrations of HB-EPS in Types 1, 2 and 3 mats, compared to low concentrations in Yellow fur and pudding mats, is consistent with high wave resistance and greater biomass for the classic smooth mats, and low wave resistance for the diatom and pudding mats.

The mats fall into two different groupings with respect to their carbohydrate profiles. Mat types 1, 2 and 3 have high total extracted carbohydrate concentrations; this material is dominated by cEPS and HB-EPS. The yellow fur and coccoid pudding mats had high biomass in the upper surface, but a high proportion of carbohydrate in these mats was not EPS, but either cLMW or HW extracts. This suggests a more active photosynthetic biomass, but probably high turnover times (either by physical removal or metabolic activity), preventing the accumulation of significant quantities of structural EPS. The dynamics of the carbohydrates in these fractions is not known. The values reported in this paper represent only one point in time; and mat concentrations are likely subject to diel and other temporal changes. These changes could be investigated with tracer studies.

Developing an Ecological Framework for Stromatolite Formation

The three "classic" surface microbial mat communities originally described by Reid et al. (2000), result in the deposition of three different sediment types (e.g., accreted ooids, micritic crust, fused grain layer). As such each community/sediment type represent different "morphological phenotypes" in an ecological sense. The more than ten years of temporal observations have revealed that the three "classic" mat communities do not exist in isolation. Rather, the surface mats are subjected to periodic/intermittent colonization by a number of other mat forming organisms including diatoms. This temporary colonization results in the formation of several intermittent communities of different species composition. Further, the colonization by these communities, may either enhance, compromise or confound the formation of laminae during stromatolite formation. It is not yet know whether eukaryote attempts at colonization may challenge the existing bacterial communities of stromatolites, or may contribute signatures that may be preserved at depth.

These observations present the exciting possibility that periodic invasion by the accessory species and resulting variability that is generated, are likely important to the cycling and broader ecological stability of the stromatolites, and may contribute to stromatolite formation. Further, it is possible to begin developing an empirically testable ecological framework for understanding stromatolite formation. We hypothesize here that the three "classic" mat types (Types 1, 2, and 3 mats) constitute "alternate stable states" (sensu May, 1977; Knowlton, 1992). The concept of an "alternate state" is used in ecology to describe biological communities that possess inherent resiliency, but may change to a different "state" (or basin of attraction) when exposed to a larger (i.e., threshold-dependent) disturbance, which causes an irreversible change in the system (May, 1977, Knowlton, 1992). Evidence that has accumulated from a variety of different ecological systems now support the alternate state idea. The hypothesis posits that several alternate (community) states may exist, which cycle back and forth. Each community is relatively stable (over time) in response to minor perturbations (i.e., disturbances that do not invoke a net change in species). However, when a major disturbance occurs, the community may shift to a new stable state having different members, and/or relative abundances of species, or the disturbance may cause a shift to an entirely new community.

The alternate stable state hypothesis is potentially testable, especially when using the microbial communities of stromatolites, since testing requires that the communities remain relatively stable over several generations during exposure to perturbations - something that is not possible when using slow-growing species. We further hypothesize that colonization by eukaryote communities represents an intermediate disturbance, one that is under different selective pressures (i.e., more sensitive to burial). Elucidation of stromatolite formation will require an understanding of the ecological processes and community changes occurring over different temporal scales. The present study provides an initial descriptive foundation for testing these hypotheses.

CONCLUSIONS

1. Four major microbial mat communities colonize the surfaces of the modern marine stromatolites at Highborne Cay: (1) the "classic" Type 1 (*Schizothrix* mats), Type 2 (Biofilm mats), and Type 3 (*Solentia* mats) mats as described in Reid et al. (2000), (2) stalked diatom mats (consisting mainly of *Licmophora* and *Striatella* species), (3) tube diatom mats (stringy pustules and pustular blanket consisting of Naviculid – like tube-forming diatoms) and (4) pudding mats (pale pudding and coccoid pudding, dominated by species of *Phormidium* and *Cyanothece*).

2. The newly described diatom and pudding mats augment "classic" Type 1 mats by contributing to ooid trapping on the surface of the stromatolites.

3. Clustering of mat types based on DGGE analyses is consistent with the groupings based on field and microscope descriptions. The stalked diatom mats group together, and are related to the "classic" mats. The tube diatom mats cluster together, as do the pudding mats, and these two groups are distinct from the "classic" mats.

4. The carbohydrate profiles distinguish between the "classic" mat types and the other surface communities. Type 1, 2 and 3 mats have high total extracted carbohydrate concentrations; this material is dominated by structural EPS - both cEPS and HB-EPS. In contrast, the dominant carbohydrate in the yellow fur stalked diatom mats and coccoid pudding mats is cLMW or HW extract. High amounts of structural EPS contribute to high wave resistance (e.g., Type 1, 2, and 3 mats), whereas low concentrations result in mats that exhibit low wave resistance and are easily eroded (e.g., diatom mats, pudding mats).

5. Stromatolites, by nature of their different sediment composition and microbial communities involved in their deposition, may provide a model system for testing the alternate stable state hypothesis.

ACKNOWLEDGEMENTS

The authors wish to thank the participants of RIBS past and present, the crew of the R/V Walton Smith for logistics, and the owners and residents of Highborne Cay. The work was supported in part by a grant from the NSF Biocomplexity Program (BE/CBC-0221796). This is RIBS contribution #55.

REFERENCES

Abdullahi, A.S., Underwood, G.J.C., Gretz, M.R.
2006. Extracellular matrix assembly in diatoms (Bacillariophyceae). V. Environmental effects of polysaccharide synthesis in the model diatom *Phaeodactylum tricornutum*. *Journal of Phycology* 42:363-378.

Al-Thukair, A.A., and S. Golubic
1996. Characterization of *Hyella caespitosa* var. arbuscula var. nov. (Cyanophyta, Cyanobacteria) from shoaling ooid sand grains, Arabian Gulf. *Nova Hedwigia, Beiheft* 112:81-89.

Andres, M.S., and R.P. Reid
2006. Growth Morphologies of Modern Marine Stromatolites: A Case Study from Highborne Cay, Bahamas. *Sedimentary Geology* 185:319-328.

Baumgartner, L.K., R.P. Reid, C. Dupraz, A.W. Decho, D.H. Buckley, J.R. Spear, K.M. Przekop, and P.T. Visscher
2006. Sulfate reducing bacteria in microbial mats: changing paradigms, new discoveries, *Sedimentary Geology* 185:131-145.

Baumgartner, L.K., C. Dupraz, D.H. Buckley, J.R. Spear, N.R. Pace, and P.T. Visscher
2009. Microbial species richness and metabolic activities in hypersaline microbial mats: potential role in mineral biosignature formation. *Astrobiology* (in press)

Bellinger B.J., A.S. Abdullahi, M.R. Gretz, and G.J.C. Underwood
2005. Biofilm polymers: Relationship between carbohydrate biopolymers from estuarine mudflats and unialgal cultures of benthic diatoms. *Aquatic Microbiology and Ecology* 38:169-180.

Braissant, O., A.W. Decho, K.M. Przekop, K.M. Gallagher, C. Glunk, C. Dupraz, P.T. Visscher
2009. Characteristics and turnover of exopolymeric substances (EPS) in a hypersaline microbial mat. *FEMS Microbiology Ecology* 67:293-307.

Chiovitti, A., P. Molino, S.A. Crawford, R. Teng, T. Spurck, and R. Wetherbee
2004. The glucans extracted with warm water from diatoms are mainly derived from intracellular chrysolaminaran and not exttracellular polysaccharides. *European Journal of Phycology* 39:117-128.

Burns, B.P., Goh, F., Allen, M., and B.A. Neilan
2004. Microbial diversity of extant stromatolites in the hypersaline marine environment of Shark Bay, Australia. *Environmental Microbiology* 6:1096-1101.

Decho, A.W.
2000. Exopolymer microdomains as a structuring agent for heterogeneity within biofilms. Pages 9-15 in R.E. Riding and S.M. Awramik (eds.) *Microbial Sediments*, Springer

Desnues, C.G., B. Rodriguez-Brito, S. Rayhawk, S. Kelley, T. Tran, M. Haynes, H. Liu, D. Hall, F.E. Angly, R.A. Edwards, R.V. Thurber, R.P. Reid, J. Siefert, V. Souza, D. Valentine, B. Swan, M. Breitbart, and F. Rohwer
2008. Biodiversity and biogeography of phages in modern stromatolites and thrombolites. Nature 452:340-345.

Dill, R.F., E.A. Shinn, A.T. Jones, K. Kelly, and R.P. Steinen.
1986. Giant sub-tidal stromatolites forming in normal salinity waters. *Nature* 324:55-58

Dravis, J.
1983. Hardened subtidal stromatolites, Bahamas. *Science* 219:385-386.

Dupraz, C., P.T. Visscher, L.K. Baumgartner, and R.P. Reid
2004. Microbe-mineral interactions: early carbonate precipitation in a hypersaline lake (Eleuthera Island, Bahamas). *Sedimentology* 51:745-765.

Dupraz, C.D., and P.T. Visscher
2005. Microbial lithification in marine stromatolites and hypersaline mats. *Trends in Microbial Ecology* 13:429-438.

Eckman J.E., M.S. Andres, R.L. Marinelli, E. Bowlin, R.P. Reid, R.J. Aspden, and D.M. Paterson
2008. Wave and sediment dynamics along a shallow sub-tidal sandy beach inhabited by modern marine stromatolites. *Geobiology* 6:21-32.

Foster. J.S., S.J. Green, S.R. Ahrendt, S. Golubic, R.P. Reid, K.L. Hetherington, and L. Bebout
2009. Molecular and morphological characterization of cyanobacterial diversity in the stromatolites of Highborne Cay, Bahamas. *The ISME Journal* 3:573-587.

Franks, J., R.P. Reid, R.J. Aspen, G.J.C. Underwood, D.M. Paterson, L. Prufert-Bebout, and J.F. Stolz
2009. Ooid accreting diatom communities from the modern marine stromatolites at Highborne Cay, Bahamas. Pages (in press) in J. Seckbach and A. Oren (eds), *Microbial Mats*, Springer

Gektidis, M., and S. Golubic
1996. A new endolithic cyanophyte/cyanobacterium: *Hyella vacans* sp. nov. from Lee Stocking Island, Bahamas. *Nova Hedwigia, Beiheft* 112:91-98.

Golubic, S., and K.M. Browne
1996. *Schizothrix gebeleinii* sp. nov. builds subtidal stromatolites, Lee Stocking Island, Bahamas. *Algological Studies* 83:273-290.

Golubic, S., L. Seong-Joo, and K.M. Browne
2000. Cyanobacteria: architects of sedimentary structures. Pages 57-67 in R.E. Riding and S.M. Awramik (eds.) *Microbial Sediments*, Springer

Hanlon, A.R.M., B. Bellinger, K. Haynes, G. Xiao, G., T.A. Hofmann, M.R. Gretz, A.S. Ball, A.M. Osborn, and G.J.C. Underwood
2006. Dynamics of EPS production and loss in an estuarine, diatom-dominated, microalgal biofilm over a tidal emersion immersion period. *Limnology and Oceanography* 51:79-93.

Havemann, S.A., and J.S. Foster
2008. Comparative characterization of the microbial diversities of an artificial microbialite model and a natural stromatolite. *Applied and Environmental Microbiology* 74:7410-7421.

Haynes, K., T.A. Hofmann, C.J. Smith, A.S. Ball, G.J.C. Underwood, and A.M. Osborn
2007. Diatom-Derived Carbohydrates as Factors Affecting Bacterial Community Composition in Estuarine Sediments. *Applied and Environmental Microbiology* 73:6112-6124.

Knowlton, N.
1992. Thresholds and multiple stable states in coral-reef community dynamics. *American Zoologist* 32:674-682.
Ley, R.E., J.K. Harris, J. Wilcox, J.R. Spear, S.R. Miller, B.M. Bebout, J.A. Maresca, D.A. Bryant, M.L. Sogin, and N.R. Pace
2006. Unexpected diversity and complexity of the Guerrero Negro hypersaline microbial mat. *Applied and Environmental Microbiology* 72:3685-3695
Littler, D.S., M.M. Littler, I.G. Macintyre, E. Bowlin, M.S. Andres, and R.P. Reid
2005. Guide to the dominant macroalgae of the stromatolite fringing reef complex, Highborne Cay, Bahamas. *Atoll Research Bulletin* 532:67-91.
López-Córtez, A, F. García-Pichel, U. Nuebel, and R. Vázquez-Juárez
2001. Cyanobacterial diversity in extreme environments in Baja California, Mexico: a polyphasic study. *International Microbiology* 4:434-442
Macintyre, I.G., L. Prufert-Bebout, and R.P. Reid
2000. The role of endolithic cyanobacteria in the formation of lithified laminae in Bahamian stromatolites. *Sedimentology* 47:915-921.
May, R.M.
1977. Thresholds and breakpoints in ecosystems with a multiplicity of stable states. *Nature* 269:471-477.
Muyzer, G., S. Hottentrager, A. Teske, and C. Wawer
1996. Denaturing gradient gel electrophoresis of PCR-amplified 16S rDNA-A new molecular approach to analyse the genetic diversity of mixed microbial communities. Pages 3.4.4:1–23 in A.D.L. Akkermans, J.D. van Elsas, and F. J. De Bruijn (eds.), *Molecular Microbial Ecology Manual*, Kluwer Academic Publishing
Paterson, D.M., R.J. Aspden, P.T. Visscher, M. Consalvey, M.S. Andres, A.W. Decho, J. Stolz, and R.P. Reid
2008. Light dependent biostabilisation of sediments by stromatolite assemblages. *PloS One* 3:e3176
Perkins, R.G., J.C. Kromkamp, and R.P. Reid
2007. Importance of light and oxygen for photochemical reactivation in photosynthetic stromatolite communities after natural sand burial. *Marine Ecology Progress Series* 349:23-32.
Reid, R.P., I.G. Macintyre, R.S. Steneck, K.M. Browne, and T.E. Miller
1995. Stromatolites in the Exuma Cays, Bahamas: Uncommonly common. *Facies* 33:1-18.
Reid, R.P., P.T. Visscher, A.W. Decho, J.F. Stolz, B.M. Bebout, C. Dupraz, I.G. Macintyre, H.W. Paerl, J.L. Pinckney, L. Prufert-Bebout, T.F. Steppe, and D.J. DesMarais
2000. The role of microbes in accretion, lamination and lithification of modern marine stromatolites. *Nature* 406:989-992.
Rothrock Jr. M.J., and F. García-Pichel
2005. Microbial diversity of benthic mats along a tidal desiccation gradient. *Environmental Microbiology* 7:593-601
Seong-Joo, L., K.M. Browne, and S. Golubic
2000. On stromatolite lamination. Pages 16-24 in R.E. Riding and S.M. Awramik (eds.) *Microbial Sediments*, Springer

Smith, D.J., and G.J.C. Underwood
1998. Exopolymer production by intertidal epipelic diatoms. *Limnology and Oceanography* 43:1578-1591
Stolz, J.F, T.N. Feinstein, J. Salsi, and R.P. Reid
2001. Microbial role in sedimentation and lithification in a modern marine stromatolite: a TEM perspective. *American Minerologist* 86:826-833.
Stolz, J.F.
2003. Structure in marine biofilms. Pages 65-76 in W.E. Krumbein, D.M. Paterson, and G.A. Zavarzin (eds.) *Fossil and Recent Biofilms- a natural history of life on Earth* Kluwer Academic Publishers
Visscher, P.T., R.P. Reid, B.M. Bebout, S.E. Hoeft, I.G. Macintyre, and J. Thompson Jr.
1998. Formation of lithified micritic laminae in modern marine stromatolites (Bahamas): the role of sulfur cycling. *American Mineralogist* 83:1482-1491.
Visscher, P.T., R.P. Reid, and B.M. Bebout
2000. Microscale observations of sulfate reduction: correlation of microbial activity with lithified micritic laminae in modern marine stromatolites. *Geology* 28:919-922.
Visscher, P.T., S.E. Hoeft, T.M.L. Surgeon, D.R. Rogers, B.M. Bebout, J.S. Jr. Thompson, and R.P. Reid
2002. Microelectrode measurements in stromatolites: Unraveling the Earth's past? Pages 265-282 in M. Taillefert and T. Rozan (eds), ACS Symposium Series 220. *Environmental Electrochemical Analyses of Trace Metal Biogeochemistry*, Cambridge University Press
Underwood, G.J.C., D.M. Paterson, and R.J. Parkes
1995. The measurement of microbial carbohydrate exopolymers from intertidal sediments. *Limnology and Oceanography* 40:1243-1253
Underwood, G.J.C. and J. Kromkamp
1999. Primary production by phytoplankton and microphytobenthos in estuaries. *Advances in Ecological Research* 29:93-153.
Underwood, G.J.C.
2001. "Microphytobenthos" Pages 1770-1777 in J Steele, S. Thorpe, and K. Turekian (eds), Encyclopedia of Ocean Sciences, Academic Press
Underwood, G.J.C.
2002. Adaptations of tropical marine microphytobenthic assemblages alonga gradient of light and nutrient availablilty in Suva Lagoon, Fiji. *European Journal of Phycology* 37:449-462
Underwood, G.J.C., M. Boulcott, C.A. Raines, and K. Waldron
2004. Environmental effects on exopolymer production by marine benthic diatoms – dynamics, changes in composition and pathways of production. *Journal of Phycology.* 40:293-304.
Wustman, B.A., M.R. Gretz and K.D. Hoagland
1997. Extracellular matrix assembly in diatoms (Bacillariophyceae) I. A model of adhesives based on chemical characterization and localization of polysaccharides from the marine diatom *Achnanthes longipes* and other diatoms. *Plant Physiology* 113:1059-1069.